Journal of Mathematical Chemistry 15 (1994) 323–337

Electronic structure of random copolymers

Kyozaburo Takeda

NTT Basic Research Laboratories, Musashino, Tokyo 180, Japan

Received 18 February 1993; revised 10 August 1993

The electronic structure of random copolymers (RCP) is theoretically investigated by the single-site coherent potential approximation. The results are also compared with those by the band calculation for the corresponding ordered system. In the $A_{1-x}B_x$ binary RCP, a strong reduction in the system band gap ($E_g(A_{1-x}B_x)$) is found in the dilute B region when the system has the relation of $E_g(A) > E_g(B)$. This dependence is caused by the asymmetric quenching in the density-of-states (DOS) singularity at the band-edge states. The gap-opening mechanism and the asymmetric quenching are discussed by focusing on the role of the spatial dimension on the electronic structure of the random system, and the theoretical treatment is finally applied to the calculation of the joint DOS for the Si–Ge RCP system.

1. Introduction

Although copolymers are the fundamental form of polymers, their electronic structures are not yet fully understood. This is because normal copolymers do not have the ordered arrangement of the component elements (ordered copolymer, OCP), but have the disordered arrangement (random copolymer, RCP). Pioneering theoretical considerations on this aperiodicity in the RCP systems have been extensively carried out by Ladik's group and Del Re's group. Ladik and Seel [1] first discussed the self-consistent field (SCF) treatment of a periodic polymer containing a cluster of impurities, and constructed the disordered chain's Fock matrix from the Fock matrices of the periodic systems by introducing the chemical building block technique (CBBT) [2]. They calculated the density-of-state (DOS) energy profile of large finite polymers by employing algorithms like the negative factor counting (NFC) method of Dean [3]. They applied their treatment to investigate the electronic structures of biopolymers [4]. Ladik also developed the application of the Green function approach to this field [5]. With Del Re, he gave the general analysis of the local impurity SCF approach [6] and applied it to quasi-one-dimensional systems [7].

The characteristic features of the electronic properties in the low dimensional systems including polymers and copolymers originate from the DOS singularity at the band-edges. The purpose of the present work is to investigate the electronic

characteristics in the RCP systems, focusing on how the randomness in the RCP causes the DOS singularity to vary, compared with that of the OCP system. For this purpose, the coherent potential approximation (CPA) method [8–10] is employed. The reasons are that the disordering in the RCP system is (and/or can be reduced to be) the typical site-substitutional randomness in the backbone atoms and that the CPA method revealed the electronic characteristics due to this type of randomness [10]. Moreover, the CPA method is not limited to the finite systems but applicable to the infinite system, and is independent to the numbers of the components. Therefore, with the help of the CPA method, it is possible to systematically investigate the electronic structure of the "huge and/or infinite" RCP as well as the finit RCP.

In section 2, we describe the application of the CPA method to the RCP systems, and reform the coupled linear-complex equations for the multi-component RCP system. The results for the binary RCP are discussed in section 3.1. The investigation is further extended to the multi-component (ternary and quaternary) RCP systems in section 3.2 and also to the actual system of the Si–Ge RCP in section 3.3.

2. Theoretical calculation

2.1. DOS FOR THE RANDOM SYSTEM

The DOS $N(E)$ is given by

$$N(E) = -\frac{1}{\pi} \lim_{\eta \to 0} \mathrm{Im}\{\mathrm{Tr}[G(E + \mathrm{i}\eta)]\}, \tag{1}$$

where the Green function G of the system is known. For random systems, however, the system's Hamiltonian, i.e., the system's Green function, is not uniquely defined. In this case, the DOS ($N^{\mathrm{rdm}}(E)$) can be expressed by ensemble-averaging of the DOS for the individual random configuration sets. Since this ensemble-averaging and the tracing of the Green function matrix are exchangeable for the system involving many ensembles, the $N^{\mathrm{rdm}}(E)$ can be expressed as

$$N^{\mathrm{rdm}}(E) = \langle N(E) \rangle = -\frac{1}{\pi} \lim_{\eta \to 0} \mathrm{Im}(\mathrm{Tr}[\langle G(E + \mathrm{i}\eta) \rangle]), \tag{2}$$

and is determined by calculating the trace of the ensemble averaged Green function $\langle G \rangle$.

The ensemble averaged Green function ($\langle G \rangle$) is defined by the effective Hamiltonian H_{eff}, as

$$\langle G \rangle = (Z\mathbf{1} - H_{\mathrm{eff}})^{-1}, \tag{3}$$

where the effective Hamiltonian H_{eff} is expressed in terms of the site-expression form,

$$H_{\text{eff}} = \sum |i\rangle\sigma\langle i| + \sum |i\rangle v_{ij}\langle j| , \tag{4}$$

where σ is the coherent potential energy for the random system and v_{ij} is the transfer energy from the ith site to the jth site. The sum should be carried out over the all sites.

We, now, introduce the function $F_0(Z)$ by using the following equation:

$$F_0(Z) = \frac{1}{N}\sum_{\lambda} \frac{1}{Z - \epsilon_\lambda} . \tag{5}$$

The trace of the ensemble averaged Green function, $\text{Tr}[\langle G\rangle]$, can be obtained by multiplying the system's total site number N by F_0 as follows:

$$\text{Tr}[\langle G\rangle] = NF_0(E - \sigma) . \tag{6}$$

This is because the trace ($\text{Tr}[\langle G\rangle]$) is given in terms of the site (λ) expression as

$$\text{Tr}[\langle G\rangle] = \sum_{\lambda} \langle\lambda|\langle G\rangle|\lambda\rangle = \sum \frac{1}{E - \sigma - \epsilon_\lambda} . \tag{7}$$

Thus, instead of calculating $\text{Tr}[\langle G\rangle]$ directly, we can obtain the DOS for the random system by calculating the imaginary part of F_0.

2.2. CALCULATION OF F_0 FUNCTION

Here, we limit the random copolymer (RCP) to a system, whose backbone atoms are randomly substituted with several atoms [11]. In this system, it is possible to determine the DOS energy profile for each homopolymer because each homopolymer has an ordered arrangement of the component substance. Let us consider how the function F_0 can be expressed for the RCP in terms of the DOS (N_0) for each homopolymer.

Since the DOS for the pure substrate (N_0) is defined as

$$N_0(\epsilon) = \sum_{k} \delta(\epsilon - \epsilon_k) , \tag{8}$$

the function $F_0(E - \sigma)$ can be obtained by using this N_0,

$$F_0(E - \sigma) = \frac{1}{N}\int_{-\infty}^{\infty} \frac{N_0(\epsilon)}{(E - \sigma) - \epsilon}\, \mathrm{d}\epsilon . \tag{9}$$

In the 1D ordered homopolymer system, the singularity in the DOS energy profile at the band-edges is most characteristic. The present aim is to investigate the characteristic features of the electronic structure for the RCP systems, focusing on how the DOS singularities are influenced by the randomness. The aim can be

fully discussed, by using the free electron approach with the effective mass approximation. The DOS of the 1D homopolymer (N_0^{1D}) is then given by the following equation:

$$N_0^{1D}(E) = \begin{cases} \dfrac{N}{4}\dfrac{1}{\sqrt{1-E}}(-1<E<0), \\ \\ \dfrac{N}{4}\dfrac{1}{\sqrt{1+E}}(0<E<1), \end{cases} \tag{10}$$

where E is the reduced energy in units of half-bandwidth energy. Substituting eq. (10) for N_0 in eq. (9), the F_0 function for the RCP having the coherent potential σ can be analytically expressed as follows:

$$F_0^{1D}(E-\sigma) = \frac{1}{4}\left[\frac{2\tan^{-1}\dfrac{1}{\sqrt{E-\sigma-1}}}{\sqrt{E-\sigma-1}} - \frac{\ln\dfrac{1-\sqrt{E-\sigma+1}}{1+\sqrt{E-\sigma+1}}}{\sqrt{E-\sigma+1}} - i\frac{\pi}{\sqrt{E-\sigma+1}}\right]. \tag{11}$$

It is also important to compare the results for the 1D RCP with the results for the 2D and 3D random alloy systems, because the singularity in the DOS energy profile strongly depends on the spatial dimension. Since another purpose of this paper is to consider the role of the spatial dimension in the electronic structure of the random systems, similar investigations were carried out for the 2D and 3D random systems.

The DOS of the ordered pure 2D and 3D substances ($N_0^i, i = 2D$ and 3D) are given by

$$N_0^{2D}(E) = \frac{N}{2}(-1<E<1), \tag{12}$$

$$N_0^{3D}(E) = \frac{2}{\pi}N\sqrt{1-E^2}(-1<E<1). \tag{13}$$

The corresponding F_0 functions are then given by

$$F_0^{2D}(E-\sigma) = \frac{1}{2}\ln\frac{E-\sigma+1}{E-\sigma-1}, \tag{14}$$

$$F_0^{3D}(E-\sigma) = 2\left(E-\sigma-\sqrt{(E-\sigma)^2-1}\right). \tag{15}$$

2.3. S-CPA CONDITION

The remaining problem is to determine the coherent potential energy σ of the RCP. Since we focus on the site-substitutional randomness, the coherent potential

energy is obtained by the CPA condition. For simplicity, we consider here the single-site coherent potential approach (S-CPA) [10], whose condition for the multi-component system involving n elements is

$$\sum C_i \frac{\epsilon_i - \sigma}{1 - (\epsilon_i - \sigma)F_0(E - \sigma)} = 0\,, \tag{16}$$

where the symbols C_i and ϵ_i are the content ratio and the on-site energy of the ith element (see appendix).

Since the F_0 function is given as a functional form of σ, both σ and F_0 should be determined self-consistently by coupling the S-CPA condition (eq. (16)) and the function F_0 (eqs. (11), (14) or (15)). We solve these values numerically by Muller's method for the complex non-linear coupled equations [12].

3. Results and discussion

3.1. BINARY RCP SYSTEM

Figure 1 shows the DOS energy profile of the 1D binary RCP. On-site energies used in the calculation are $E_A = -1$ and $E_B = 1$ in units of half-bandwidth energy, and the composition ratio is $C_A = C_B = 0.5$. The characteristic features are an energy-gap opening at the center of energy ($E \sim 0$) and also a strong quenching of the DOS singularity at these gap-edge states.

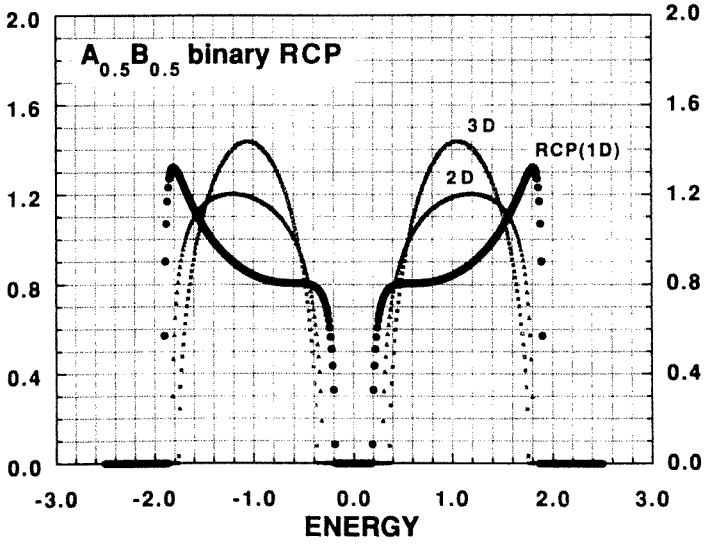

Fig. 1. DOS energy profiles for $A_{0.5}B_{0.5}$ binary RCP. On-site energies of elements A and B are $E_A = -1$ and $E_B = 1$ (energy unit is half-bandwidth). The results for 2D and 3D random systems are also shown.

First, let us investigate the gap-opening, based on the comparison with the band structure of the 1D homopolymer. For the pure substances of homopolymer A and B, the corresponding $E - k$ dispersion should be as shown in fig. 2. When these two elements are mixed to form a binary ordered copolymer (OCP) A_1B_1, what happens to the electronic structure? This system has a lattice vector twice that of each original pure substance. The band structure of the resulting binary OCP roughly corresponds to the half (folded into halves, i.e., 1/2) zone-folded band of the pure original substance.

When the binary RCP system has the on-site energies of $E_A = -1$ and $E_B = 1$ and also if the transfer energy between the element A and B is zero, an accidental degeneracy occurs between the antibonding state of the element A and the bonding state of the element B, i.e., the simple half zone-folding of the Brillouin zone (BZ). This transfer energy, however, is finite, because these two elements should mix to form a copolymer. Orbital mixing then occurs between the two accidentally degenerated states, and they are split into the final bonding and antibonding state to cause a gap-opening. The gap-opening in the random system basically occurs by this orbital mixing.

Figure 1 also shows the DOS energy profiles for the random alloy systems of other dimensions (2D and 3D). It is found that the RCP (1D) has the smallest gap-opening and this gap-opening increases with the increase in the spatial dimension. This characteristic can be understood by counting the neighboring site numbers. The RCP has two neighboring sites because of its one-dimensionality. The other dimensional random system has more site numbers, e.g., 4 or 6 sites for the 2D square or 3D cubic lattice, respectively. In the random system, the atomic arrangement is, however, not uniquely determined. Only the composition ratio is defined through ensemble-averaging. Therefore, the higher dimensional random system has a larger probability of placing the heterogeneous atoms at the neighboring sites. According to the gap-opening mechanism mentioned above, a larger gap

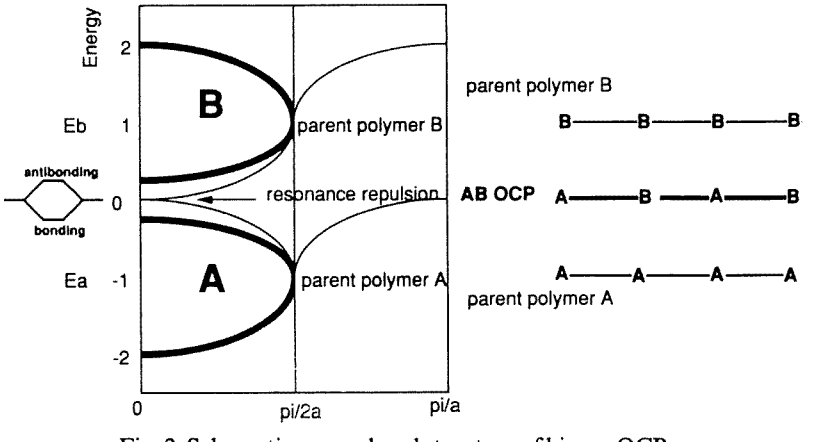

Fig. 2. Schematic energy band structure of binary OCP.

should open when more heterogeneous atoms are positioned at the neighboring sites. Thus, the higher dimensional random system has the larger gap-opening.

This feature is a characteristic of the random system. Within the Hückel approximation, the gap-opening for the ordered system is equally conserved independent of the spatial dimension (band-gap limitation). This limitation originates from the spatial symmetry in the superlattice system. Table 1 summarizes the calculated band gaps for both random and ordered systems and the corresponding tail-states. The band-tail grows with decrease in the dimension.

We explain this gap-limitation by considering the case of the 2D square binary ordered system. All the nearest neighboring sites in this 2D binary square lattice are occupied by heterogeneous atoms (simple superlattice). For a comparison with the results by the S-CPA method, the following are also assumed: The transfer energies are limited between the nearest neighbor bonds (Hückel approach). The values of the on-site energies and the transfer energies used in the band calculations are the same as those used in the CPA calculations and each atom has a spherical symmetric wave function.

The band structure of this simple 2D superlattice is obtained from the following LCAO secular equations.

$$\begin{vmatrix} \alpha - E & 2t\cos k_x a/2 & 2t\cos k_y a/2 & 0 \\ 2t\cos k_x a/2 & \beta - E & 0 & 2t\cos k_y a/2 \\ 2t\cos k_y a/2 & 0 & \beta - E & 2t\cos k_x a/2 \\ 0 & 2t\cos k_y a/2 & 2t\cos k_x a/2 & \alpha - E \end{vmatrix} = 0 . \tag{17}$$

Here, α and β are the on-site energies of the atoms A and B, respectively, and t is the transfer energy between them.

The factor group of this 2D square binary superlattice is isomorphous with the point group D_{2d}. The unit cell of this superlattice includes two atoms of each substance A and B. Four states should, therefore, appear and those at point Γ are expressed in terms of the irreducible representations of A_g, B_{2u} and B_{3u} (fig. 3). The two A_g states correspond to the bonding state for the four s-like AOs and the antibonding state between them, respectively.

The band gap of this system is determined by the highest occupied valence band (HOVB) state (B_{2u}) and the lowest unoccupied conduction band (LUCB) state (B_{3u}). Since the only atoms located diagonally in the unit cell give the net orbital

Table 1
Energy gaps of random (E_g^{rdm}) and ordered (E_g^{ord}) systems and tail-states ($\Delta E = (E_g^{ord} - E_g^{rdm})/2$). Values are in units of half-bandwidth.

Dimensionality	E_g^{rdm}	E_g^{ord}	ΔE
1D	0.38	2	0.81
2D	0.58	2	0.71
3D	0.72	2	0.64

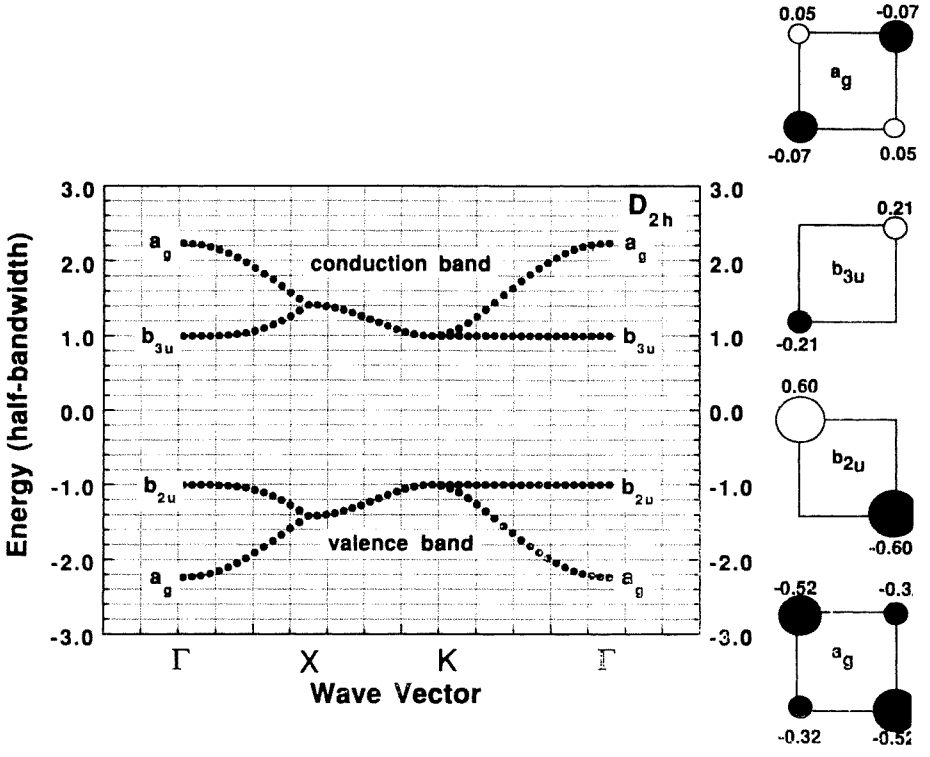

Fig. 3. Band structure of 2D binary RCP ordered square superlattice. On the right hand side, the orbital characters at point Γ are also shown.

contribution to these band-edge states, orbital mixing does not occur between the nearest neighbor sites and the resulting band-edge states are left with localizing, i.e., band-gap limitation.

Due to the structural symmetry, the same limitation in the gap-opening occurs in the other dimensional (1D and 3D) ordered systems. Thus, within the Hückel approach, the gap-opening is independent of the spatial dimension. On the other hand, the random system has no structural symmetry, and has the possibility of placing the homogeneous atoms at the nearest neighbor site. These neighboring atoms cause the additional orbital mixings, which destabilize the HOVB state and stabilize the LUCB state and cause the tail-states. Thus, the gap-limitation disappears in the random system.

Figure 4 shows the DOS energy profile of the binary RCP $A_{0.6}B_{0.4}$ ($C_A = 60\%$, $C_B = 40\%$). The DOS singularity of the element B completely disappears due to the site-substitutional randomness. Moreover, singularity-quenching occurs asymmetrically in the energy. A large amount of the quenching occurs in the energy of the A–B mixing region. This asymmetric quenching is weakened when the system's dimension is increased: In the 2D system, the asymmetric quenching is reduced more than that in the 1D system [13]. Since the 3D system inherently has no singu-

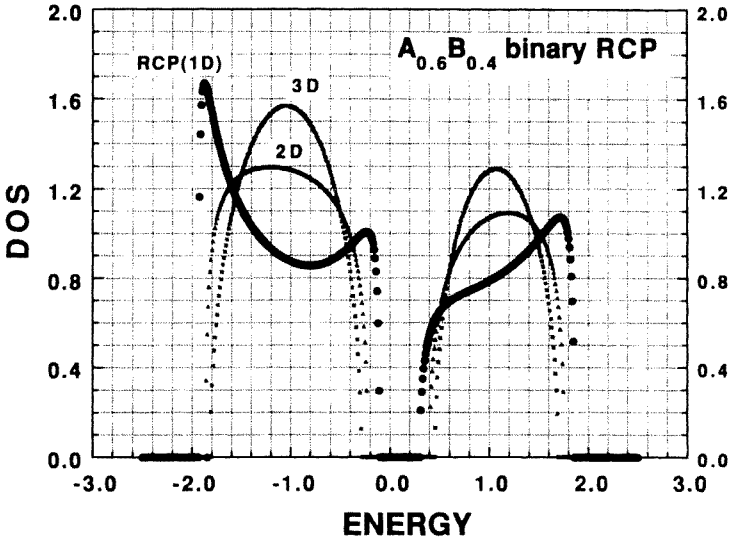

Fig. 4. DOS energy profiles for $A_{0.6}B_{0.4}$ binary RCP. On-site energies of elements A and B are $E_A = -1$ and $E_B = 1$ (energy unit is half-bandwidth). The results for 2D and 3D random systems are also shown.

larity, the singularity-quenching does not occur. Therefore, the 3D system maintains the symmetric energy profile even when the randomness is introduced.

The present characteristics, e.g., the asymmetric quenching of the DOS singularity and the gap-opening of the RCP system etc. have been also reported by the other theoretical methods of the CBBT-NFC approach by Ladik's group [2,7] and the Green function approach by Del Re et al. [6,7]. Ladik et al. obtained the corresponding energy spectrum of the large but finite chains by the NFC method [2], and found the similar electronic characteristics for the virtual finite proteins including 20 glycine and serine amino-acid groups. They also found that these features are characterized more clearly with the increase of the polymerization. The limiting results for the infinite chains by Del Re et al. [7] well approach the present ones.

Following Onodera and Toyozawa [14], we characterize the electronic structure of the RCP system by the value of the gap-opening: If gap > 0, the original characters of each substance are not mixed, and the system becomes a persistence type. If gap $= 0$, the alloying annihilates the original characteristics of each substance, and an amalgamation type system appears. Figure 5 shows the boundary of the persistence and the amalgamation types of the binary RCP. Since the 1D RCP has the smallest gap-opening in every dimension, the 1D system tends to be the amalgamation type, provided that the alloying content and the on-site energies are the same.

3.2. MULTI-COMPONENT RCP SYSTEMS

The DOS energy profile of the multi-component RCP can be also interpreted by the above BZ folding scheme. Figure 6 shows the DOS energy profile of the tern-

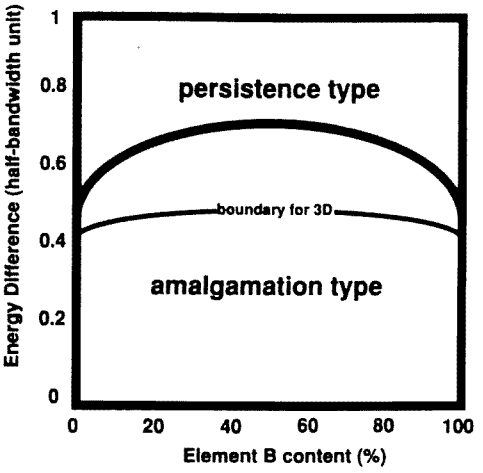

Fig. 5. Type of alloying in A_xB_{1-x} binary RCP system. ΔE means $|E_A - E_B|/2$ in half-bandwidth units. The result for the 3D system is also shown.

ary RCP ($A_{0.25}B_{0.25}C_{0.25}$, on-site energies of $E_A = -1, E_B = 0, E_C = 1$ in units of half-bandwidth energy). If the binary RCP is formed by the elements A and C, the gap-opening should occur at $E = 0$. However, by adding element B to form the ternary RCP, the DOS of the element B exists finitely at $E = 0$, and compensates the gap-opening due to the mixing of the elements A and C. Therefore, the gap-opening disappears in the resulting DOS of $A_{0.25}B_{0.5}C_{0.25}$.

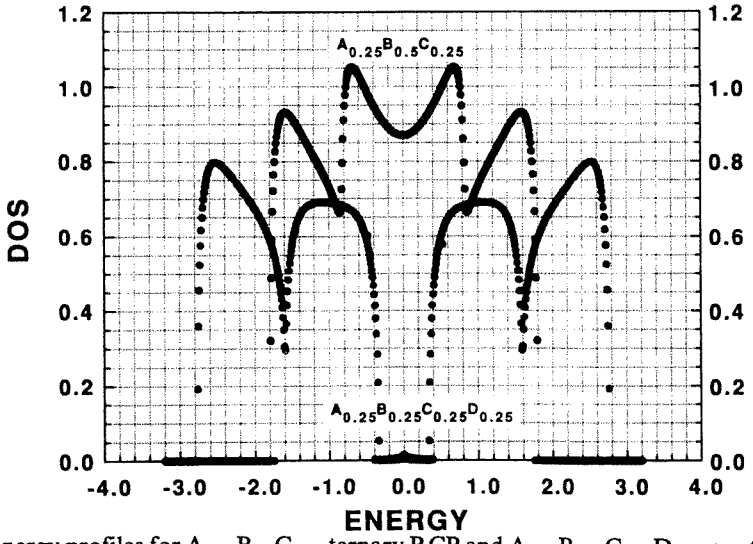

Fig. 6. DOS energy profiles for $A_{0.25}B_{0.5}C_{0.25}$ ternary RCP and $A_{0.25}B_{0.25}C_{0.25}D_{0.25}$ quaternary RCP. On-site energies of elements A, B and C are $E_A = -1, E_B = 0$ and $E_C = 1$ for ternary RCP and for elements A, B, C and D $E_A = -2, E_B = -1, E_C = 1$ and $E_D = 2$ for quaternary RCP (energy unit is half-bandwidth).

In one case the element number of the substances plays an essential role in the gap-opening. Figure 6 also shows the result for the quaternary RCP ($A_{0.25}B_{0.25}C_{0.25}D_{0.25}$, $E_A = -2, E_B = -1, E_C = 1, E_D = 2$). Significant resonance repulsion remains between elements B and C, and the actual gap-opening separates the resulting system into the apparent two systems of AB and CD amalgamation, although all substances are mixed equally.

The unequal distribution of the DOS is also a characteristic of the 1D multi-component RCP systems, because the quenching of the DOS singularity increases in the energy region ($E \sim 0$) where more resonance-repulsions occur but the total DOS should be conserved. Therefore, the resulting DOS tends to increase in both elements that have the lowest and highest on-site energies; i.e., the elements A and D of this case. This unequal distribution contrasts strongly with 3D random systems, in which the DOS distribution is conserved equally if all substances are mixed equally. Thus, the RCP system consisting of an even number elements tends to produce a gap-opening and become a persistence type. On the other hand, an amalgamation type tends to be produced in the RCP system consisting of an odd number elements and the resulting DOS is maldistributed.

3.3. APPLICATION TO Si–Ge RCP SYSTEM

The following are the considerations for the Si–Ge RCP system. This system [15,16] is suitable for the application of the S-CPA method for the following reasons.

- Si–Ge RCP has a site-substitutional randomness in the backbone.
- The electronic structures of the parent homopolymers, polysilane (PSi) and polygermane (PGe), are quite resemble each other. Both have the directly allowed type band structure at point Γ.
- The electronic states at the band-edges are well delocalized along the skeleton and the effective mass approximation is possible.

We calculate the joint density-of-states (JDOS) for the Si–Ge RCP system, because the JDOS represents the electronic structure near the Fermi level and directly corresponds to the optical absorption spectrum. The JDOS of the parent homopolymer (i = PSi or PGe) can be expressed by the effective mass approximation as follows:

$$g_i^{\mathrm{JDOS}}(E) = \begin{cases} \dfrac{1}{2\pi}\left(\dfrac{2m_i^*}{\hbar^2}\right)^{1/2} \dfrac{1}{\sqrt{E - E_g^i}} \left(E_g \leqslant E \leqslant E_g + \dfrac{W}{2}\right), \\ \dfrac{1}{2\pi}\left(\dfrac{2m_i^*}{\hbar^2}\right)^{1/2} \dfrac{1}{\sqrt{E_g^i + W - E}} \left(E_g + \dfrac{W}{2} \leqslant E \leqslant E_g + W\right). \end{cases} \tag{18}$$

Here E_g^i is the band gap and m_i^* is the reduced effective mass defined as,

$$\frac{1}{m_i^*} = \frac{1}{m_i^{\text{elec}}} + \frac{1}{m_i^{\text{hole}}} .$$

The symbol W is the first JDOS band width of PSi and PGe. This value is nearly equal for PSi and PGe because of the similarity of their electronic structures.

By transforming the energy E into $\epsilon = E - E_g^i - W/2$ in units of $W/2$ energy, eq. (18) corresponds to eq. (10). The discussion in section 3.1 is therefore capable of the JDOS calculation for the Si–Ge RCP system. The band parameters of PSi and PGe used in the present work are determined by first principle band calculations [17].

Figure 7 shows the band-edge JDOS energy profile of $Si_{0.9}Ge_{0.1}$ RCP. Pure PSi causes the JDOS singularity at 3.9 eV and pure PGe causes it at 3.3 eV. These singularities are quenched by the randomly distributed "impurity" Ge atom. Particularly in this case, the low Ge content strongly quenches the singularity due to PGe, as if annihilates it. Consequently, the vestige of PGe's singularity overlaps with PSi's JDOS and forms the tail-state. This tail-state grows toward the lower energy region with the increase of Ge content and changes to be a divergent form when the RCP includes the higher Ge content. At the same time, the singularity due to PSi, however, disappears so as to conserve the value of the total density. This band-edge JDOS energy profile is also important to discuss the fundamental optical absorption edge of the Si–Ge RCP system, if the system has the weak energy dependence in the optical transition matrix elements.

Figure 8 compares the band gap E_g of the Si_xGe_{1-x} RCP system with that of the Si_mGe_n OCP system [17]. The E_g values for the RCP system were obtained by the CPA calculation of JDOS, and the values for the OCP system were obtained by

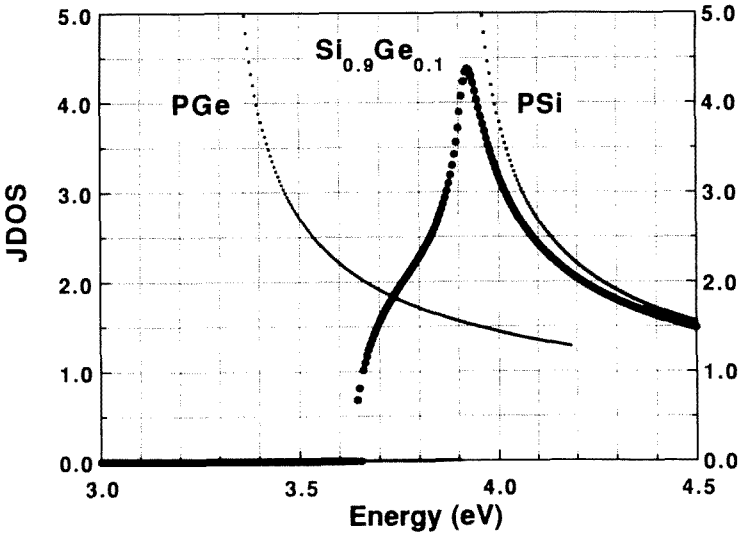

Fig. 7. JDOS energy profile of $Si_{0.9}Ge_{0.1}$ RCP near the band-edge. Those for pure PSi and PGe are also shown in figure.

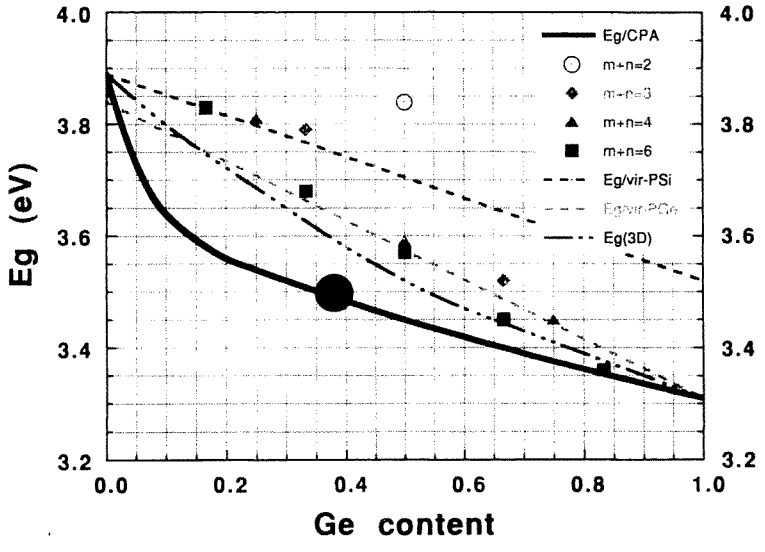

Fig. 8. Dependence of E_g on Ge content in SiGe RCP system. E_g for the ordered Si_mGe_n systems is also shown in the figure. The large solid circle is the experimental result of $Si_{1.6}Ge_1$ RCP. The broken line and the shaded broken line are the results by the virtual crystal approximation.

the first principle band calculation for the Si_mGe_n supercells [17]. In the Si_mGe_n OCP system, the value of E_g depends on the length of Si catenation (or Ge catenation), even when the OCPs have the same composition ratio, e.g., the OCP molecules of Si_1Ge_2 and Si_2Ge_4 have the same Ge content (33%), but the theoretical E_g values have a difference about 1 eV. It should be, however, pointed out that the E_g values of these OCP molecules stand within those predicted by the virtual SiGe atom copolymer [18].

On the other hand, the E_g values of the RCP molecules shown in fig. 8 differ considerable from those of the virtual atom approximation. A significant decrease in E_g values is found, particularly, in the dilute Ge region. This strong bowing in the dependence of E_g on composition is a characteristic of the 1D RCP system, and is found in real Si_xGe_{1-x} RCP system. An 11% reduction in the E_g value is found when the Ge parts are copolymerized by 38% [15]. This value agrees well with the theoretical prediction of a 10.2% reduction (fig. 8). A similar strong reduction has been also observed in the other 1D RCP system, e.g. the $Se_{1-x}Te_x$ system [19,20].

This strong reduction in E_g is weakened with the increase in dimension, because this feature is caused by the largest tail-states due to asymmetric quenching of DOS singularity in the 1D random system. Figure 8 also shows the E_g composition dependence of the hypothetical 3D random Si–Ge system, whose pure substances are assumed to have the same E_g values as those of PSi and PGe but the 3D character is assumed in the DOS profile. The dependence of E_g on composition varies more gradually and uniformly, because the 3D random system has no asymmetric quenching.

Acknowledgements

The author would like to express his thanks to Profs. Mitsuru Fukuchi and Fumiko Yonezwa of Keio University for their many fruitful discussions on the CPA theory. He thanks Prof. Haruo Hosoya of Ochyanomizu University for his valuable discussion on the gap-limitation mechanism. Also, he thanks Drs. Kenji Shiraishi of NTT, Takao Watanabe of SONY and Kyoko Nakada of Ochyanomizu University for their helpful comments.

Appendix

By transforming the S-CPA condition (eq. (16)) into the polynomial form by using $F_0 = F_0(E - \sigma)$, one can gain a clear insight into the application to multi-component systems. The resulting polynomial forms of binary, ternary and quaternary alloy systems are given.

- Binary alloy system

$$aF_0 + b = 0\,,$$

$$a = -(E_A - \sigma)(E_B - \sigma)\,,$$

$$b = C_A E_A + C_B E_B - \sigma\,. \tag{19}$$

- Ternary alloy system

$$aF_0^2 + bF_0 + c = 0\,,$$

$$a = (E_A - \sigma)(E_B - \sigma)(E_C - \sigma)\,,$$

$$b = -\,[(C_A + C_B)(E_A - \sigma)(E_B - \sigma) + (C_B + C_C)(E_B - \sigma)(E_C - \sigma) + (C_C + C_A)(E_C - \sigma)(E_A - \sigma)]\,,$$

$$c = C_A E_A + C_B E_B + C_C E_C - \sigma\,. \tag{20}$$

- Quaternary alloy

$$aF_0^3 + bF_0^2 + cF_0 + d = 0\,,$$

$$a = -(E_A - \sigma)(E_B - \sigma)(E_C - \sigma)(E_D - \sigma)\,,$$

$$b = (1 - C_D)(E_A - \sigma)(E_B - \sigma)(E_C - \sigma) + (1 - C_A)(E_B - \sigma)(E_A - \sigma)(E_D - \sigma)$$

$$+ (1 - C_B)(E_C - \sigma)(E_D - \sigma)(E_A - \sigma)$$
$$+ (1 - C_C)(E_D - \sigma)(E_A - \sigma)(E_B - \sigma),$$

$$= - C_A(E_A - \sigma)(E_B - \sigma) - C_A(E_A - \sigma)(E_C - \sigma) - C_A(E_A - \sigma)(E_D - \sigma)$$
$$- C_B(E_B - \sigma)(E_C - \sigma) - C_B(E_B - \sigma)(E_D - \sigma) - C_B(E_B - \sigma)(E_A - \sigma)$$
$$- C_C(E_C - \sigma)(E_D - \sigma) - C_C(E_C - \sigma)(E_A - \sigma) - C_C(E_C - \sigma)(E_B - \sigma)$$
$$- C_D(E_D - \sigma)(E_A - \sigma) - C_D(E_D - \sigma)(E_B - \sigma) - C_D(E_D - \sigma)(E_C - \sigma),$$

$$d = C_A E_A + C_B E_B + C_C E_C + C_D E_D - \sigma. \tag{21}$$

References

[1] J. Ladik and M. Seel, Phys. Rev. 13 (1976) 5338.
[2] R.S. Day, K. Suhai and J. Ladik, Chem. Phys. 62 (1981) 165.
[3] P. Dean, Rev. Mod. Phys. 44 (1972) 127.
[4] There are many theoretical works by Ladik's group; e.g., R.S. Day, S. Suhai and J. Ladik, Chem. Phys. 62 (1981) 165;
J. Ladik, M. Seel, P. Otto and A.K. Bakhsi, Chem. Phys. 108 (1986) 203, 215, 223, 233.
[5] J. Ladik, Phys. Rev. B17 (1978) 1663.
[6] G. Del Re and J. Ladik, Chem. Phys. 49 (1980) 321.
[7] M. Seel, G. Del Re and J. Ladik, J. Comp. Chem. 3 (1982) 451.
[8] P. Soven, Phys. Rev. 156 (1967) 809.
[9] D.W. Taylor, Phys. Rev. 156 (1967) 1017.
[10] Review e.g.: F. Yonezawa and K. Morigaki, Prog. Theor. Phys. Suppl. 53 (1973) 1.
[11] Even for the side-chain substitutional RCP, the side-chain randomness can be effectively reduced to the change in the backbone potential.
[12] D.E. Müller, Math. Tables and Aids to Comput. 10 (1956) 208.
[13] Clearly the flat-profile in the DOS energy dependence disappears.
[14] Y. Onodera and F. Toyozawa, J. Phys. Soc. Jpn. 24 (1968) 341.
[15] P. Trefonas and R. West, J. Poly. Sci. Poly. Chem. Edit. 23 (1985) 2099.
[16] H. Isaka, M. Fujiki, M. Fujino and N. Matumoto, Macromol. 24 (1991) 2467.
[17] K. Takeda, K. Shiraishi and N. Matumoto, J. Am. Chem. Soc. 112 (1990) 5043.
[18] The Si_1Ge_1 alternating OCP gives an irregular large value because this copolymer is the only exception having no pure Si–Si and Ge–Ge bonds.
[19] A.K. Bhatnager and S.V. Subrahmayan, Solid State Commun. 42 (1982) 281.
[20] T. Yamaguchi and F. Yonezawa, J. Non-Crys. Solids 117/118 (1990) 324.